

## Surface-phonon calculations for the Al(110) surface

K. M. Ho

*Ames Laboratory, U.S. Department of Energy, and Department of Physics, Iowa State University, Ames, Iowa 50011*

K. P. Bohnen

*Kernforschungszentrum Karlsruhe, Institut für Nukleare Festkörperphysik, Postfach 3640, D-7500 Karlsruhe 1, Federal Republic of Germany*

(Received 19 July 1988)

The frequencies of surface modes at high-symmetry points of the surface Brillouin zone have been calculated with interplanar surface force constants determined from first-principles self-consistent total-energy calculations for the Al(110) surface. The multilayer relaxation for this surface produces big deviations of the surface force constants from the bulk values.

### I. INTRODUCTION

Surface vibrations play an important role in various dynamical processes on surfaces at ambient or elevated temperatures. Although theoretical studies of surface vibrational waves go back to the early work of Rayleigh in the previous century,<sup>1</sup> it is only very recently, with the development of high-resolution electron-energy-loss spectroscopy<sup>2-4</sup> and inelastic helium beam scattering experiments,<sup>5,6</sup> that we have the capability of accurately measuring the surface-phonon dispersion curves. Interpretation of these new data revealed the need for further theoretical work. Theoretically surface-phonon dispersion curves can be obtained by solving for the vibrational modes of a slab or semi-infinite crystal. Early calculations<sup>7</sup> modeled the interatomic interactions by a Lennard-Jones potential. Subsequent studies<sup>8-11</sup> used more realistic force constants deduced from fitting experimental bulk-phonon dispersion curves. Empirical adjustments of the surface force constants were made to reproduce the measured surface mode frequencies. However, it was found that the changes necessary are very model dependent: two different models reproducing the same bulk-phonon dispersion curves may require very different changes in parameters to reproduce the same surface modes, giving rise to very different physical interpretations.<sup>11</sup> It is obvious that a determination of the surface force constants from first principles would be very useful in interpreting experimental data and guiding experimental investigations on unmeasured crystal surfaces.

First-principles local-density-functional total-energy calculations have been very successful in determining bulk structural and vibrational properties in a variety of materials. Applications of the same techniques to surfaces are now feasible with advances in the speed of computers. In this paper, we report on a study on the surface phonons on the Al(110) surface using first-principles self-consistent total-energy calculations. From our results we obtained interplanar force constants which allowed us to determine the surface-phonon modes and surface-phonon density of states for wave vectors at high-symmetry

points of the surface Brillouin zone (SBZ). In Sec. II we will describe details of the calculation. Results will be presented in Sec. III and compared with experiment<sup>6</sup> and other calculations.<sup>12</sup>

### II. CALCULATION

Self-consistent pseudopotential calculations were performed for the Al(110) surface and the total energy of the system evaluated within the local-density-functional formalism<sup>13</sup> using the Wigner interpolation formula<sup>14</sup> for the electronic exchange and correlation energy. In these calculations, the surface is modeled by periodic slabs 15 layers thick separated by five layers of vacuum. The norm-conserving pseudopotential used is the same as in previous calculations.<sup>15</sup> The electronic wave functions are expanded in a basis set containing plane waves up to a cutoff energy of 8.5 Ry, and additional plane waves with energy up to 12.0 Ry are included with second-order perturbation. Sampling grids for the surface calculations correspond to a grid of 35 points in the irreducible part of the SBZ of the (1×1) surface. Partial occupation of states near the Fermi level is taken into account by a Gaussian smearing scheme with a broadening width of 0.20 eV. For each geometry, in addition to the total energy, the forces exerted on each atom are calculated using the Hellmann-Feynman theorem,<sup>16,17</sup> these force calculations are essential for the efficient calculation of surface force constants. The inclusion of extra plane waves by second-order perturbation improves the convergence of the basis set but creates some modifications in the evaluation of forces. This is described in more detail in the Appendix. The convergence of our force and energy calculations with respect to basis-set size, slab thickness, and **k**-point sampling have been checked carefully and reported in our earlier paper.<sup>15</sup>

The choice of the Al(110) surface is motivated by previous work<sup>15</sup> in which we have accurately determined the equilibrium geometry of the Al(110) surface. We found a contraction of the top interlayer spacing by (6.8±0.5)%, an expansion of the second interlayer spacing by (3.5±0.5)%, and contraction of the third interlayer spac-

ing by  $(2.0 \pm 0.5)\%$ . Our calculated interlayer separations are in agreement with results from precise low-energy electron diffraction (LEED) experiments<sup>18,19</sup> to within 0.02 Å.

To determine the surface phonons at a particular wave vector  $q_{\parallel}$  in the SBZ, we evaluated the phonon dynamical matrix for a thick slab of 301 Al(110) layers. The interplanar force-constant matrices coupling the inner layers of the slab can be obtained from bulk calculations or from experimental bulk-phonon dispersion curves measured by inelastic neutron scattering.<sup>20</sup> The force-

constant matrices coupling the surface layers are evaluated by first-principles calculations using the 15-layer periodic slab geometry. Starting with the equilibrium geometry, the surface layer is distorted slightly with small atomic displacements corresponding to the surface wave vector  $q_{\parallel}$ . Self-consistent calculations are then performed for the distorted surfaces and the forces induced on the various atoms in the slab are calculated. Since part of the translational symmetry of the system parallel to the surface is destroyed, a bigger unit cell is required for the calculations with distortion. Thus, the first-

TABLE I. Interplanar force-constant matrices coupling the top two surface layers to other layers for surface wave vectors at high-symmetry points in the surface Brillouin zone. Units are  $10^4$  dyn/cm. Also shown for comparison are the corresponding interplanar force constants obtained from bulk-phonon dispersion curves and from our first-principles calculation for the interior layers of our slab. Matrix elements not listed are zero by symmetry.

		Surface			Bulk	Interior of slab
$q_{\parallel} = \bar{\Gamma}$						
(1x, 2x)	2.08	(2x, 3x)	1.23		1.49	1.43
(1y, 2y)	5.03	(2y, 3y)	3.22		4.06	3.80
(1z, 2z)	1.67	(2z, 3z)	1.44		1.75	1.75
(1x, 3x)	0.17	(2x, 4x)	0.19		0.23	0.22
(1y, 3y)	-0.09	(2y, 4y)	-0.10		-0.25	-0.28
$q_{\parallel} = \bar{X}$						
(1x, 1x)	-9.57	(2x, 2x)	-11.59		-11.81	
(1y, 1y)	-5.39	(2y, 2y)	-7.44		-6.51	
(1z, 1z)	-5.36	(2z, 2z)	-4.61		-7.29	
(1x, 2z)	2.43	(2x, 3z)	1.97		2.40	
(1z, 2x)	2.72	(2z, 3x)	1.90		2.40	
(1x, 3x)	-0.40	(2x, 4x)	-0.24		-0.26	
(1y, 3y)	-0.03	(2y, 4y)	-0.25		-0.39	
(1z, 3z)	2.72	(2z, 4z)	1.72		1.79	
$q_{\parallel} = \bar{Y}$						
(1x, 1x)	-2.38	(2x, 2x)	-2.51		-2.83	-2.82
(1y, 1y)	-4.80	(2y, 2y)	-9.05		-7.92	-7.46
(1z, 1z)	-4.61	(2z, 2z)	-5.57		-7.64	-7.34
(1y, 2z)	3.61	(2y, 3z)	2.67		3.18	2.76
(1z, 2y)	3.46	(2z, 3y)	2.49		3.18	2.76
(1x, 3x)	0.19	(2x, 4x)	-0.08		0.06	0.13
(1y, 3y)	0.30	(2y, 4y)	-0.02		-0.15	-0.27
(1z, 3z)	2.90	(2z, 4z)	1.91		2.39	2.32
$q_{\parallel} = \bar{S}$						
(1x, 1x)	-9.53	(2x, 2x)	-11.25		-11.71	
(1y, 1y)	-4.97	(2y, 2y)	-7.97		-7.93	
(1z, 1z)	-5.57	(2z, 2z)	-5.42		-7.14	
(1x, 2y)	3.63	(2x, 3y)	2.45		3.35	
(1y, 2x)	3.64	(2y, 3x)	2.37		3.35	
(1x, 3x)	0.09	(2x, 4x)	-0.01		-0.08	
(1y, 3y)	0.16	(2y, 4y)	0.20		0.28	
(1z, 3z)	2.75	(2z, 4z)	1.63		2.24	

principles calculations are only computationally feasible for surface wave vectors at the zone center or high-symmetry points in the SBZ.

Calculations for successive displacements in three orthogonal directions [ $x$ , (1-10);  $y$ , (001);  $z$ , (110)] determine the force-constant matrices coupling the surface layer with the neighboring layers. Diagonalization of the dynamical matrix yields all the vibrational modes of the slab with wave vector  $\mathbf{q}_{\parallel}$ . Surface-phonon and surface-resonance modes can be determined by analyzing the eigenvectors looking for modes with big amplitudes at the surface.

### III. RESULTS

In Table I, we present the results of our calculated force-constant matrices coupling the first and second surface layers to other layers for surface wave vectors at the center  $\bar{\Gamma}$  and the  $\bar{X}$ ,  $\bar{Y}$ , and  $\bar{S}$  points of the SBZ. The asymmetric force-constant matrices indicate that the forces acting at the surface are noncentral in character. Shown in the third column are the corresponding bulk force-constant matrices obtained from the measured bulk-phonon dispersion curves.<sup>20</sup> For the wave vectors  $\bar{\Gamma}$  and  $\bar{Y}$ , we have calculated the interplanar force constants coupling the fifth layer of our 15-layer slab to its neighbors. The results, shown in column 4, are very close to the values obtained by using bulk force constants. For most of the important matrix elements, there is a trend for an enhancement in magnitude for force constants coupling the surface layer to its neighbors and a decrease in magnitude for the coupling of the second layer to the

inner layers when compared with the bulk force-constant matrix elements. The physical origin of this effect is the large multilayer relaxation present on the Al(110) surface which brings the topmost surface layer inward and the second layer outward.

Our results for the surface-phonon frequencies are summarized in Table II. The displacements of the surface layer for the surface modes are also listed. The subscript 2 included with the surface polarization indicate that the displacement of that mode is zero in the first layer and localized instead on the second layer with the given direction. Results are presented considering changes in surface force constants coupling the top and second surface layers and for changes in only the topmost layer.<sup>21</sup> Inclusion of changes in second layer couplings has insignificant effects on almost all the modes, except for the  $y$  modes at  $\mathbf{q}_{\parallel} = \bar{Y}$  which are pushed up due to a strong stiffening of the intralayer coupling at the second layer and a slight shift of the  $y$  mode at  $\mathbf{q}_{\parallel} = \bar{S}$  into the bulk-phonon continuum. Since the changes in force constants are oscillatory because of the oscillatory pattern of the surface relaxation, we expect the real answer to lie somewhere between the two sets of numbers. Also shown for comparison in Table II are the results obtained with bulk interplanar force constants. The most dramatic effect of the changes in surface force constants is the stiffening of the two horizontal shear modes at  $\mathbf{q}_{\parallel} = \bar{X}$  and  $\mathbf{q}_{\parallel} = \bar{Y}$ . These modes are highly localized on the top layer because the displacements on the second layer are restricted to zero by symmetry. Thus, they are extremely sensitive to any changes in force constants at the surface.

To facilitate comparison with experiment, we have cal-

TABLE II. Results of surface-phonon frequencies obtained from the present calculations. The first column shows the results obtained using bulk interplanar force constants deduced from the experimental bulk phonon-dispersion curves. The second shows the result obtained by considering changes in the force-constant matrices coupling the top surface layer to the inner layers, and the third column shows the results when changes in force-constant matrices for the topmost and second surface layers are considered. Units are in meV.

	Bulk interplanar force constants	Surface interplanar force constants		Expt. (Ref. 6)
		1	1+2	
$\mathbf{q}_{\parallel} = \bar{X}$				
$z$	15.1	17.3	17.2	14.8
$x$	17.3	16.9	16.7	not measured
$y$	16.2	22.8	22.8	not measured
$z$		24.6	25.3	not measured
$y_2$		26.2	26.9	not measured
$x$	32.4	31.7	31.8	not measured
$z$	34.9			
$\mathbf{q}_{\parallel} = \bar{Y}$				
$z$	13.3	14.1	13.9	13.5
$y$	8.6	7.9	10.4	9.3
$x$	10.2	14.8	14.9	not measured
$y$	24.6	24.6	25.8	not measured
$\mathbf{q}_{\parallel} = \bar{S}$				
$z$	13.9			
$y$	14.6	15.8		
$x$	33.0	33.1	32.9	not measured

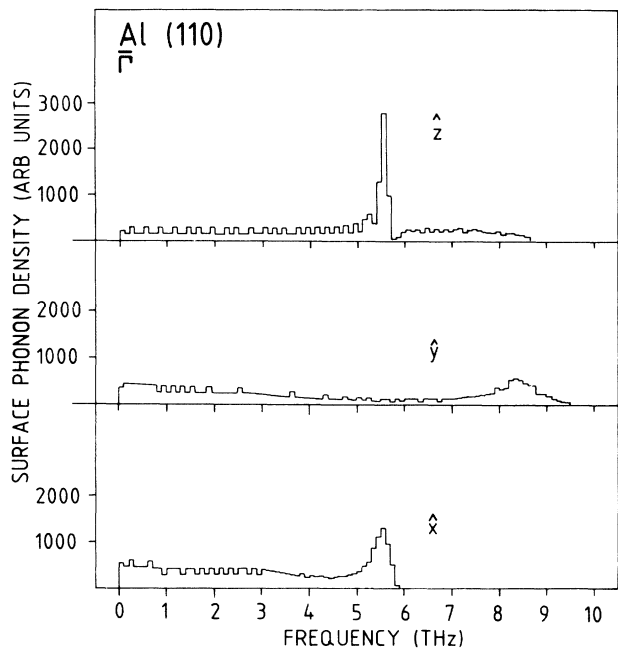


FIG. 1. The surface-phonon density of states is given for the  $\bar{\Gamma}$  point for different polarizations.  $\hat{x}$  denotes the  $(1\bar{1}0)$  direction,  $\hat{y}$  the  $(001)$  direction, and  $\hat{z}$  the  $(110)$  direction perpendicular to the surface.

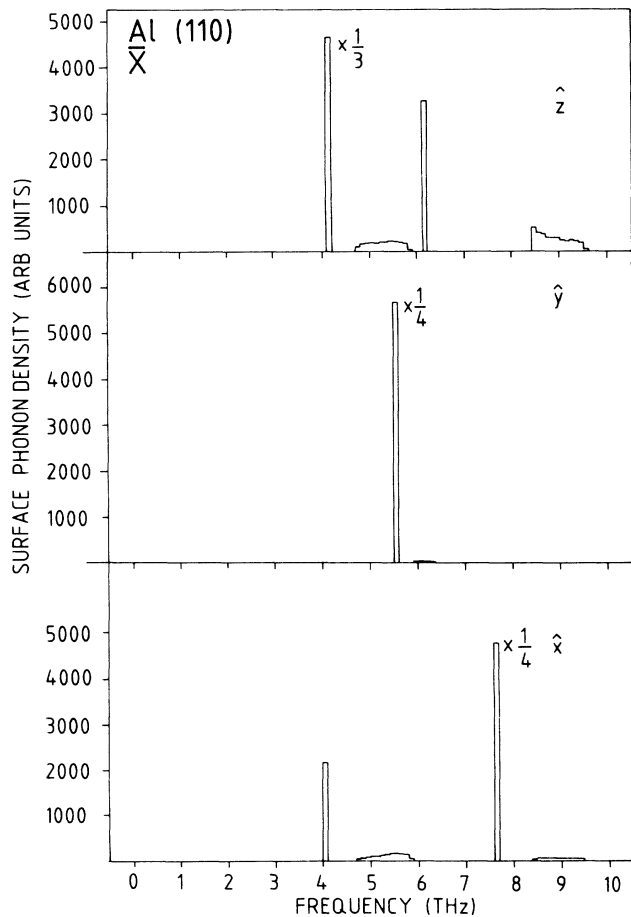


FIG. 2. Surface-phonon density of states for the  $\bar{X}$  point. The surface modes are clearly visible. For the meaning of  $\hat{x}$ ,  $\hat{y}$ , and  $\hat{z}$  see Fig. 1.

culated the surface-phonon density of states for the Al(110) surface:

$$D_{\mathbf{q}_{\parallel},\alpha}(\omega) = \sum_n \delta(\omega - \omega_n) |\mathbf{u}_{n,\mathbf{q}_{\parallel}} \cdot \hat{\mathbf{e}}_{\alpha}|^2,$$

where  $\mathbf{q}_{\parallel}$  is the surface wave vector,  $\hat{\mathbf{e}}_{\alpha}$  denotes the direction  $\hat{x}$ ,  $\hat{y}$ , or  $\hat{z}$ , and  $\mathbf{u}_{n,\mathbf{q}_{\parallel}}$  denotes the displacement of the surface atom for the  $n$ th normal mode of the slab with wave vector  $\mathbf{q}_{\parallel}$ . The results are displayed as histograms in Figs. 1-4. Inelastic helium beam scattering experiments (Ref. 6) have been performed to measure the surface-phonon dispersion curves of Al(110). Results have been reported for two surface modes at  $\bar{Y}$  and one surface mode at  $\bar{X}$ . While there is satisfactory agreement between the measured and calculated results for the surface modes at  $\bar{Y}$ , there is a big discrepancy for the mode at  $\bar{X}$ . The reason for this discrepancy is not precisely known. It may be due to the poor quality of the Al(110) surface used in the experiments,<sup>22</sup> or due to surface anharmonicity—since the surface force constants are very sensitive to the surface relaxation, if the magnitude of the surface relaxation is strongly temperature dependent, then the surface phonon at room temperature can be different from that calculated at  $T=0$ . It is unfortunate that the horizontal shear modes, which we pre-

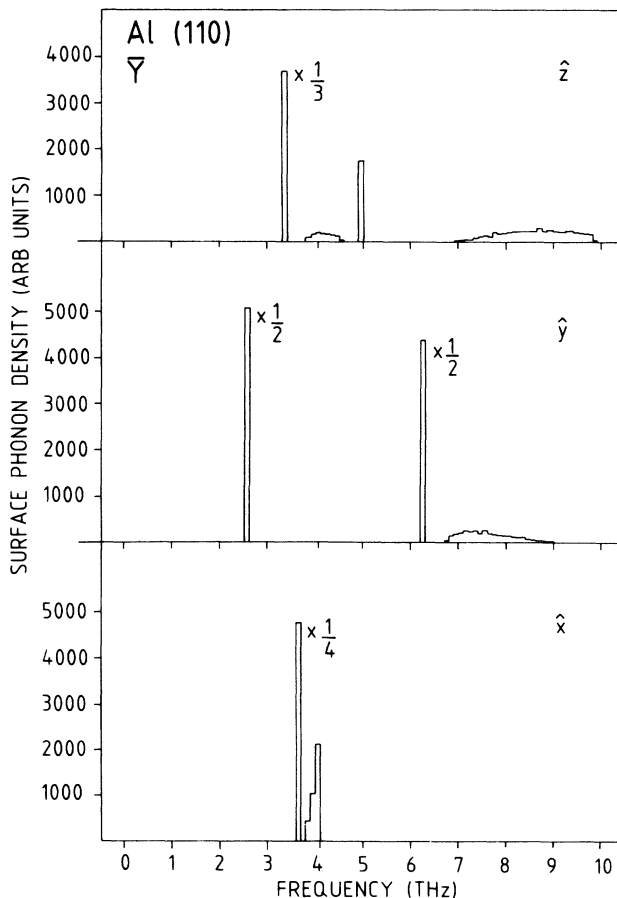


FIG. 3. Surface-phonon density of states for the  $\bar{Y}$  point.

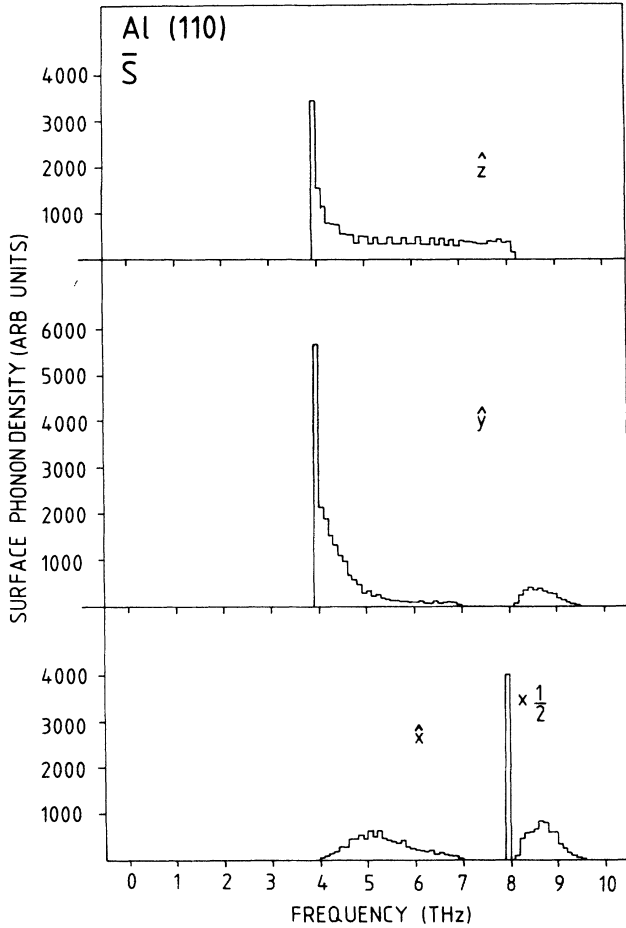


FIG. 4. Surface-phonon density of states for the  $\bar{S}$  point.

dicted to be the most surface sensitive, have not been measured because of the geometry selected for the scattering experiment.

Recently, there has been a report<sup>12</sup> of calculations of the surface-phonon dispersion curves for Al(110). These workers employed a different approach from what is used in the present calculations. Focusing on the electronic screening matrix at the surface, they were able to calculate the surface-phonon dispersion curves over the whole SBZ. However, their approach assumes a weak interaction between the ions and electrons which can be treated by perturbation at the Al(110) surface. This is a relatively untested assumption which may account for the difference between their reported results and the present calculation at high-symmetry points in the SBZ.

#### IV. CONCLUSIONS

Accurate first-principles self-consistent total-energy and interatomic force calculations have been carried out to determine the surface force constants coupling the surface layers at the Al(110) surface. The multilayer relaxation for this surface produces big deviations of the surface force constants from the bulk values particularly for the shear horizontal modes at the surface. The sensitivity of the surface force constants to surface relaxation for

this surface should make it interesting for future studies of surface anharmonicity.

#### ACKNOWLEDGMENTS

We would like to thank the Kernforschungszentrum Karlsruhe (for K.M.H.) and Ames Laboratory (for K.P.B.) for their hospitality and Dr. W. Weber, B. N. Harmon, and C. Stassis for helpful comments and discussions. Ames Laboratory is operated for the U.S. Department of Energy by Iowa State University under Contract No. W-7405-Eng-82. Part of this work is supported by the Director for Energy Research, Office of Basic Energy Sciences (including a grant of computer time on the Cray computers at the Lawrence Livermore Laboratory), and by NATO Grant No. RG(85/0516).

#### APPENDIX: CALCULATION OF THE HELLMANN-FEYNMAN FORCES FOR BASIS SETS WITH LÖWDIN FOLD-DOWN

In electronic structure calculations, it is often advantageous to improve the convergence of the chosen basis set by including the influence of a larger basis through second-order perturbation.<sup>23</sup> Such a procedure can be expressed mathematically as a folding down of the larger Hamiltonian matrix into a smaller one:

$$\tilde{H}_{ij} = H_{ij} + \sum_k \frac{H_{ik} H_{kj}}{\bar{\epsilon} - H_{kk}}$$

Here  $H_{ij}$  indicates the Hamiltonian matrix elements for members of the small basis set. The summation in  $k$  runs over the extra basis set functions included with second-order perturbation and  $\bar{\epsilon}$  is an estimate of the average eigenvalue.

While this folding-down procedure reduces the time spent in matrix diagonalization, it does introduce additional modifications in the calculation of Hellmann-Feynman forces. The details are described below. Following the derivation in an earlier paper<sup>17</sup> the expression for the Hellmann-Feynman force can be written as

$$\mathbf{F} = \mathbf{F}_{\text{ion}} + \mathbf{F}_{\text{el}},$$

$$\mathbf{F}_{\text{ion}} = - \frac{\delta \gamma_{\text{Ewald}}}{\delta \tau},$$

$$\mathbf{F}_{\text{el}} = \sum_n \left[ - \frac{\delta \epsilon_n}{\delta \tau} \right] + \int \rho \frac{\delta v_{HX}}{\delta \tau} d^3r,$$

where  $\delta \epsilon_n$  is the change in eigenvalue due to the atomic displacement  $\delta \tau$ , the summation is over all occupied states  $n$ ,  $\delta v_{HX}$  indicate the change in screening potential caused by the displacement, and  $\gamma_{\text{Ewald}}$  is the Ewald energy which measures the ion-ion interaction. We can then write

$$\mathbf{F}_{\text{el}} = \sum_n \left[ \left\langle \psi_n \left| - \frac{\delta \tilde{H}}{\delta \tau} \right| \psi_n \right\rangle + \left\langle \psi_n \left| \frac{\delta v_{HX}}{\delta \tau} \right| \psi_n \right\rangle \right],$$

where  $|\psi_n\rangle$  is the wave function of the  $n$ th eigenstate. For atomic displacements, the only changes in the Hamiltonian come from the change in ionic potential  $\delta V_{\text{ion}}$  and

the change in screening potential  $\delta v_{HX}$ . Thus,

$$\mathbf{F}_{el} = \sum_n \left[ \left\langle \psi_n \left| \frac{-\delta V_{ion}}{\delta \tau} \right| \psi_n \right\rangle + \left\langle \psi_n \left| \frac{-\delta(\tilde{H} - H)}{\delta \tau} \right| \psi_n \right\rangle \right];$$

the first term is the result obtained before in Ref. 17 and when  $V_{ion}$  is the Coulomb interaction, it reduces back to the classical Hellmann-Feynman result.<sup>16</sup> The second term is an additional small contribution to the electronic force coming from the fold-down procedure. For surface calculations where there are large cancellations between  $\mathbf{F}_{ion}$  and  $\mathbf{F}_{el}$ , inclusion of the second term improves the

accuracy of the force calculation.

While the first term requires no knowledge of  $\delta v_{HX}$ , the second term involves  $\delta V = \delta V_{ion} + \delta v_{HX}$ . In our calculations  $\delta V$  is calculated as follows:

$$\delta V = \epsilon^{-1} \delta V_{ion},$$

where  $\epsilon$  is the dielectric matrix for electronic screening. In surface calculations, it is sufficient for our accuracy to include the screening only for the lower Fourier components of the potential,  $\epsilon^{-1}$  being very close to identity for the higher Fourier components. In our calculations the dielectric matrix is usually calculated as part of the procedure in iteration to self-consistency<sup>24</sup> so actually no extra calculation of  $\epsilon$  is required.

<sup>1</sup>Lord Rayleigh, London Math. Soc. Proc. **17**, 4 (1885), reprinted in Lord Rayleigh, *Scientific Papers* (Dover, New York, 1964), Vol. 2.

<sup>2</sup>I. Ibach and D. L. Mills, *Electron Energy Loss Spectroscopy and Surface Vibrations* (Academic, New York, 1982).

<sup>3</sup>See also review article by H. Ibach and T. S. Rahman, in *Chemistry and Physics of Solid Surface*, edited by R. Vanselow and R. Howe (Springer, New York, 1984).

<sup>4</sup>M. H. Mohamed and L. L. Kesmodel, Phys. Rev. B **37**, 6519 (1988).

<sup>5</sup>See review by J. P. Toennies, J. Vac. Sci. Technol. A **2**, 1055 (1984).

<sup>6</sup>J. P. Toennies and Ch. Woell, Phys. Rev. B **36**, 4475 (1987).

<sup>7</sup>R. E. Allen, G. P. Alldredge, and F. W. de Wette, Phys. Rev. B **4**, 1648 (1971); **4**, 1661 (1971).

<sup>8</sup>G. Benedek, G. P. Brivio, L. Miglio, and V. R. Velasco, Phys. Rev. B **26**, 497 (1982).

<sup>9</sup>V. Bortolani, A. Franchini, and G. Santoro, in *Electronic Structure, Dynamics, and Quantum Structural Properties of Condensed Matter*, edited by J. T. Devreese and P. van Camp (Plenum, New York, 1985).

<sup>10</sup>T. S. Rahman, D. L. Mills, and J. E. Black, Phys. Rev. B **27**, 4059 (1983); J. E. Black, T. S. Rahman, and D. L. Mills, *ibid.* **27**, 4072 (1983).

<sup>11</sup>J. E. Black and R. F. Wallis, Phys. Rev. B **29**, 6972 (1984).

<sup>12</sup>A. G. Eguluz, A. A. Maradudin, and R. F. Wallis, Phys. Rev.

Let. **60**, 309 (1988).

<sup>13</sup>P. Hohenberg and W. Kohn, Phys. Rev. **136**, B864 (1964); W. Kohn and L. J. Sham, *ibid.* **140**, A1133 (1965).

<sup>14</sup>E. Wigner, Phys. Rev. **46**, 1002 (1934).

<sup>15</sup>K. M. Ho and K. P. Bohnen, Phys. Rev. B **32**, 3446 (1985).

<sup>16</sup>H. Hellmann, *Einführung in die Quantenchemie* (Deuticke, Leipzig, 1937); R. P. Feynman, Phys. Rev. **56**, 340 (1939).

<sup>17</sup>K. M. Ho, C. L. Fu, and B. N. Harmon, Phys. Rev. B **28**, 6687 (1983).

<sup>18</sup>J. N. Andersen, H. B. Nielsen, L. Petersen, and D. L. Adams, J. Phys. C **17**, 173 (1984).

<sup>19</sup>J. R. Noonan and H. L. Davis, Phys. Rev. B **29**, 4349 (1984).

<sup>20</sup>G. Gilat and R. M. Nicklow, Phys. Rev. **143**, 487 (1966).

<sup>21</sup>The results reported in a preliminary account of this work, K. M. Ho and K. P. Bohnen, Phys. Rev. Lett. **56**, 934 (1986), consider changes only for the surface force constants coupling the top layer.

<sup>22</sup>The experimental paper (Ref. 6) reported a high density of defects and steps on the surface. This can affect the frequency of the surface phonon at  $\bar{X}$  (see Ref. 12).

<sup>23</sup>See review article by M. L. Cohen and V. Heine, in *Solid State Physics*, edited by H. Ehrenreich, F. Seitz, and D. Turnbull (Academic, New York, 1970), Vol. 24, p. 128, and references therein.

<sup>24</sup>K. M. Ho, J. Ihm, and J. D. Joannopoulos, Phys. Rev. B **25**, 4260 (1982).